

Published in Indian Journal of Chemical Technology, Vol 13, March 2006, pp 139-143

Archived in Dspace@nitr, <http://dspace.nitrkl.ac.in/dspace>

**Prediction of bed fluctuation ratio for gas solid fluidization in cylindrical and non-cylindrical beds**

**R K Singh\* & G K Roy**

Department of Chemical Engineering

National Institute of Technology, Rourkela, # India

Abstract

Gas flow in a gas-solid fluidized bed is characterized by the predominance of bubbles. This bubbly flow exhibits considerable bed fluctuation at fluid mass velocity higher than the minimum fluidization velocity leading to instability in operation, which affects the fluidization quality adversely. In the present paper, equations have been developed for the prediction of bed fluctuation ratio for gas-solid fluidization in cylindrical and non-cylindrical (viz. semi-cylindrical, hexagonal and square) beds. A fairly good agreement has been obtained between calculated and experimental values. Based on the experiments it is concluded that, under similar operating conditions bed fluctuation ratio is maximum in case of square bed and it is least in case of semi-cylindrical bed. The fluctuation ratio becomes maximum at a particular velocity ratio  $G_f/G_{mf}$  for a particular bed and then it either decreases (due to slug formation) or remains constant at higher velocity ratio thereafter. It has also been observed that transformation from bubbling to slugging mode was latest in case of semi-cylindrical bed and earliest in case of a square one, thus providing a larger span of effective gas – solid fluidization in the bubbling regime in a semi-cylindrical bed as compared to other non-cylindrical and cylindrical beds.

Keywords: Gas-Solid Fluidization, Bed fluctuation ratio, Non-cylindrical bed.

---

\* For correspondence (E-mail: [rsingh@nitrkl.ac.in](mailto:rsingh@nitrkl.ac.in), Fax: +91-661-2472926)

Fluidization is an established fluid-solid contacting technique, which has found extensive applications in carbonization, gasification, combustion and many other industries. In spite of the many advantages claimed for the fluidization phenomenon, the efficiency and quality of large-scale and deep gas-solid fluidized beds are seriously affected by bubbling and slugging behavior, when the gas velocities are higher than the minimum fluidization velocity. Bed fluctuation ratio has been widely used to quantify fluidization quality. It is defined as the ratio of highest and lowest levels, which the top of the fluidized bed occupies for any particular gas flow rate above the minimum fluidization velocity <sup>1</sup>.

First attempt to correlate fluctuation ratio to bed characteristics was given as <sup>2</sup>

$$r = e^m \left[ \frac{(G_f - G_{mf})}{G_{mf}} \right] \quad (1)$$

The slope 'm' was related to particle diameter. Beyond certain limiting value of  $(G_f - G_{mf})/G_{mf}$ , the top oscillations are also caused by slugging. The fluctuation ratio pertaining to the slugging zone follows smoothly from non-slugging zone. Since slugging is affected by the "aspect ratio" the fluctuation ratio is dependent on this.

Bed fluctuation and bed quality being interrelated, previous investigations on quality have been aimed at development of correlations for fluctuation ratio in terms of static and dynamic parameters of the system for cylindrical<sup>3</sup>, baffled cylindrical<sup>3,4</sup> and conical beds<sup>3-6</sup> of spherical and non-spherical particles of mono-size and mixed sizes<sup>6,7</sup>. Effect of promoters and bed fluctuation in cylindrical beds<sup>8</sup> and bed fluctuation in two dimensional beds<sup>9</sup> have been studied.

Although a few qualitative explanation and quantitative expressions relating to fluidization quality have been presented in terms of some of the bed parameters for cylindrical and conical beds by the previous investigators<sup>7</sup>, their effect in case of non-columnar remain un-explored. With this end in view,

studies relating to quantification of fluidization quality in terms of fluctuation ratio for three non-columnar beds, viz. the square, semi-cylindrical and hexagonal ones have been taken up.

### Experimental procedure

The experimental setup is shown in Fig. 1. All the cylindrical and non-cylindrical beds were made of transparent acrylic resin so that the bed behaviour could be observed clearly. For uniform distribution of fluidizing medium in the bed, a calming section with glass beads was used at the entrance of the column. The dimensions of the beds used and properties of the bed materials are given in Tables 1 and 2 respectively.

A known amount of the bed material was charged to the column from the top. The reproducible static bed was obtained after fluidizing the bed gradually and allowing it to settle slowly.

The compressed dry air was admitted to the column from the constant pressure tank. The bed pressure drop and the bed heights were recorded against the gradual change of flow till the fluidization condition was obtained. In the fluidized state, as the top layer of the bed was fluctuating, both levels (maximum and minimum) and the bed pressure drop were noted against flow rate.

### Development of correlations

The correlations have been developed with the help of relevant dimensionless groups involving interacting parameters like bed height, equivalent diameter of the column, particle diameter, density of the particle, density of the fluidizing medium and fluid mass velocity.

For dimensional analysis the fluctuation ratio,  $r$ , can be related to the system parameters as follows:

$$r = f \left[ \frac{dp}{Dc}, \frac{Dc}{hs} \times \frac{\rho_f}{\rho_s}, \frac{G_f - G_{mf}}{G_{mf}} \right] \quad (2)$$

Eq. (2) can be re-written as

$$r = k \left[ \left( \frac{dp}{Dc} \right)^a \left\{ \left( \frac{Dc}{hs} \right) \left( \frac{\rho_f}{\rho_s} \right) \right\}^b \left( \frac{G_f - G_{mf}}{G_{mf}} \right)^c \right]^n \quad (3)$$

Where  $k$  is the coefficient and  $a, b, c$  and  $n$  are the exponents.

The effects of the individual groups on fluctuation ratio,  $r$  have been separately evaluated for the different conduits and values of  $a, b$ , and  $c$  have been obtained from the slope of the plots.

The values of  $k$  and  $n$  have been obtained by plotting the fluctuation ratio ( $r$ ) against the correlation factor  $\left[ \left( \frac{dp}{Dc} \right)^a \left\{ \left( \frac{Dc}{hs} \right) \left( \frac{\rho_f}{\rho_s} \right) \right\}^b \left( \frac{G_f - G_{mf}}{G_{mf}} \right)^c \right]$  as shown in Fig. 2 to 5 for different beds.

On putting the values of  $a, b, c, k$  and  $n$  in Eq. 3 for different conduits using non-spherical particles, the correlations obtained are as follows<sup>10</sup>:

For cylindrical bed:

$$r = 1.95 \left[ \left( \frac{dp}{Dc} \right)^{0.04} \left\{ \left( \frac{Dc}{hs} \right) \left( \frac{\rho_f}{\rho_s} \right) \right\}^{0.04} \left( \frac{G_f - G_{mf}}{G_{mf}} \right)^{0.05} \right] \quad (4)$$

For semi-cylindrical bed:

$$r = 2.323 \left[ \left( \frac{dp}{Dc} \right)^{0.05} \left\{ \left( \frac{Dc}{hs} \right) \left( \frac{\rho_f}{\rho_s} \right) \right\}^{0.04} \left( \frac{G_f - G_{mf}}{G_{mf}} \right)^{0.07} \right] \quad (5)$$

For hexagonal bed:

$$r = 2.3 \left[ \left( \frac{dp}{Dc} \right)^{0.06} \left\{ \left( \frac{Dc}{hs} \right) \left( \frac{\rho_f}{\rho_s} \right) \right\}^{0.05} \left( \frac{G_f - G_{mf}}{G_{mf}} \right)^{0.06} \right] \quad (6)$$

And, for square bed:

$$r = 2.55 \left[ \left( \frac{dp}{Dc} \right)^{0.09} \left\{ \left( \frac{Dc}{hs} \right) \left( \frac{\rho_f}{\rho_s} \right) \right\}^{0.04} \left( \frac{G_f - G_{mf}}{G_{mf}} \right)^{0.05} \right] \quad (7)$$

With the help of above Eqs. 4 to 7, fluctuation ratios have been calculated for other experimental data points and have been compared with their experimental values.

### **Result and discussion**

It is evident from the developed correlation that the bed fluctuation ratio is a function of four dimensionless groups viz. the excess velocity ratio, the wall effect, the aspect ratio and the density ratio. As equivalent diameter ( $D_c$ ) changes with bed configuration for identical cross-sectional area, the wall effect term,  $dp/D_c$ , in the developed correlations incorporates the effect of bed geometry. Further it is revealed that the aspect ratio alone has no appreciable effect on fluctuation ratio, hence it was combined with density ratio to get some significant effect. This is due to the fact that, the range of variable studied results in an aspect ratio value nearly unity which was due to operational constraints.

The values of bed fluctuation ratio calculated with the Eqs. 4 to 7 have been compared with their respective experimental values in Figs. 2 to 5. The mean and standard deviations for the above cases are given in Table 3. Fairly good agreement has been found to exist between calculated and experimental values. Bed fluctuation ratios have also been compared for all the conduits in Table 4. Under similar operating conditions, fluctuation ratio is maximum in case of square bed and is the least in case of semi-cylindrical bed. From the observations, it is seen that the value of fluctuation ratio becomes maximum at a particular velocity ratio  $G_f/G_{mf}$ , for a particular bed and then it either decreases or remains constant at higher velocity ratio. This type of behaviour can be attributed to the fact that corresponding to such fluid velocity the bubble diameter approaches to column diameter (actual or equivalent), initiating there by the formation of slug, which eventually reduces the bed fluctuation. It is also observed that minimum slugging velocity was maximum in case of semi-cylindrical bed and minimum in case of a square bed, providing a relatively large span of effective gas – solid fluidization in the bubbling regime for a semi – cylindrical conduit.



## Nomenclature

$d_p$ : particle diameter	[m]
$D_c$ : column diameter	[m]
$G_f$ : fluid mass velocity	[kg.hr <sup>-1</sup> .m <sup>-2</sup> ]
$G_{mf}$ : fluid mass velocity at minimum fluidization	[kg.hr <sup>-1</sup> .m <sup>-2</sup> ]
$h_s$ : static bed height	[m]
$\rho_f$ : fluid density	[kg.m <sup>-3</sup> ]
$\rho_s$ : solid density	[kg.m <sup>-3</sup> ]
$r$ : fluctuation ratio	[dimensionless]

**References**

- 1 Kunii D & Levenspiel O, Fluidization Engineering (Wiley, New York), 1969.
- 2 Leva M, Fluidization (Mc Graw Hill Book Co Inc London), 1959.
- 3 Agarwal S K & Roy G K, Inst Engrs (India), Ch-1, 68(1987), 35.
- 4 Krishnamurthy S, Murthy J S N, Roy G K & Pakala V S, Inst Engrs (India), Ch 2, 61(1981), 38.
- 5 Suryanarayana A, Murthy J S N, & Sharma K J R, Inst Engrs (India), Ch 4, 63 (1982).
- 6 Biswal K C, Sahu S, & Roy G K, Chem Eng J, 23 (1982), 97.
- 7 Singh R K, Roy G K, & Suryanarayana A, Indian Chem Engr, XXXIII, 2 (1991) , 26.
- 8 Kumar A, & Roy G K , Inst Engrs (India), Ch-1, 82 (2002) , 61.
- 9 Rhodes M, Fluidization of Particles by Fluids (Monash University, Australia), 2001.
- 10 Singh R K, Studies on Certain Aspects of Gas-Solid Fluidization in Non-cylindrical Conduits, Ph D Thesis, Sambalpur University, 1997.



**Table 1 Dimension of bed employed**

Type of bed	Cross sectional area, m <sup>2</sup>	Size/diameter, m
Cylindrical	81.07 X 10 <sup>-4</sup>	0.01016 (diameter)
Semi-cylindrical	88.50 X 10 <sup>-4</sup>	0.1501 (diameter)
Square	67.24 X 10 <sup>-4</sup>	0.082 (side)
Hexagonal	64.95 X 10 <sup>-4</sup>	0.050 (side)

**Table 2 Properties of bed materials**

Material	Types of bed	Viodage ( $\epsilon_0$ )
Dolomite	Cylindrical	0.515 to 0.550
Chromite ore	Cylindrical	0.522
Coal	Cylindrical	0.543
Sago	Cylindrical	0.437
Manganese ore	Cylindrical	0.568
Dolomite	Square	0.490 to 0.520
Chromite ore	Square	0.476
Coal	Square	0.516
Ramdana	Square	0.446
Manganese ore	Square	0.531
Dolomite	Semi-cylindrical	0.468 to 0.537
Chromite ore	Semi-cylindrical	0.546
Coal	Semi-cylindrical	0.563
Sago	Semi-cylindrical	0.467
Manganese ore	Semi-cylindrical	0.527
Urea	Semi-cylindrical	0.439 to 0.484
Dolomite	Hexagonal	0.502 to 0.547
Chromite ore	Hexagonal	0.498
Urea	Hexagonal	0.412 to 0.432
Coal	Hexagonal	0.526
Sago	Hexagonal	0.416
Manganese ore	Hexagonal	0.501

**Table 3 Mean and standard deviations for fluctuation ratio**

Sl. No.	Type of Conduits	No. of Readings	Mean Deviation	Standard Deviation
1	Cylindrical	48	7.10	14.71
2	Semi-cylindrical	58	3.81	4.50
3	Hexagonal	57	3.29	5.46
4	Square	46	6.97	17.44

**Table 4 Comparison of bed fluctuation ratio in different conduits**

Sl. No.	$(D_p/D_c)10^3$	$(D_c/h_s)X(\rho_f/\rho_s)10^4$	$(G_r-G_{mf})/G_{mf}$	Cyl.	Semi-cyl	Hexa	Sqr
1	5.9	5.04	0.25	1.07	1.03	1.11	1.12
2	5.9	5.04	0.50	1.11	1.08	1.16	1.19
3	5.9	5.04	0.75	1.13	1.11	1.19	1.23
4	5.9	5.04	1.00	1.15	1.14	1.21	1.26
5	5.9	5.04	1.25	1.16	1.15	1.22	1.28
6	5.9	5.04	1.50	1.17	1.17	1.24	1.3

Note : Cyl = Cylindrical

Hexa = Hexagonal

Sqr = Square

**Caption to figures:**

Figure 1: Experimental setup

Figure 2: Correlation plot – Cylindrical bed

Figure 3: Correlation plot – Semi-cylindrical bed

Figure 4: Correlation plot – Hexagonal bed

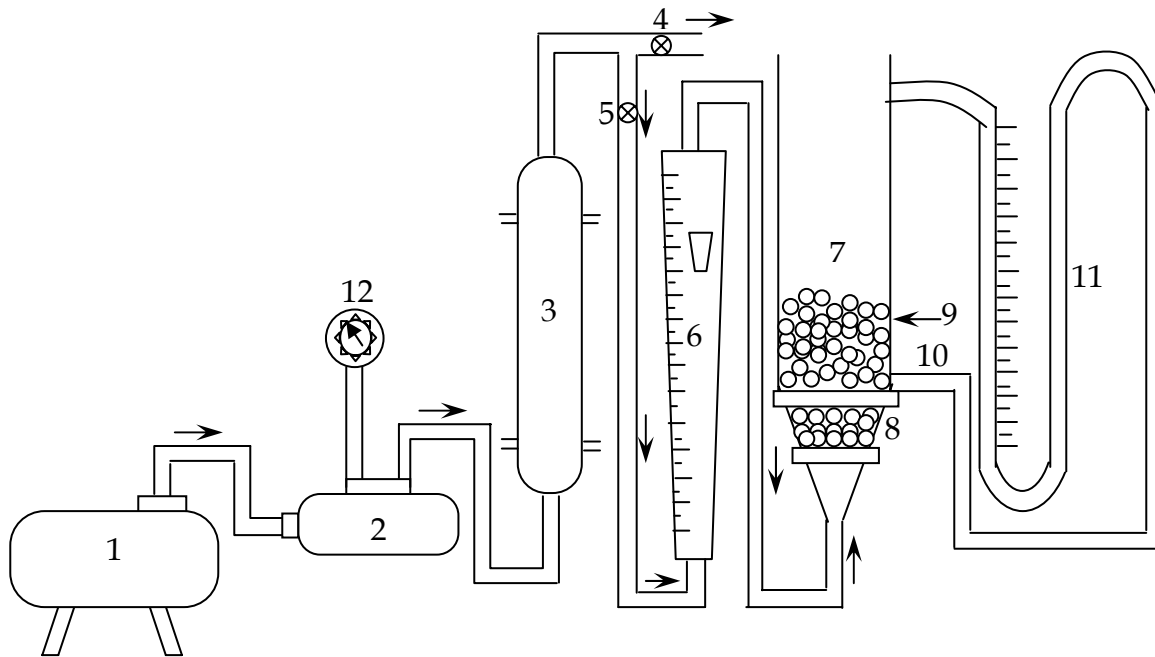
Figure 5: Correlation plot – Square bed

Figure 6: Comparison of experimental and calculated values of fluctuation ratio – Cylindrical bed

Figure 7: Comparison of experimental and calculated values of fluctuation ratio – Semi-cylindrical bed

Figure 8: Comparison of experimental and calculated values of fluctuation ratio – Hexagonal bed

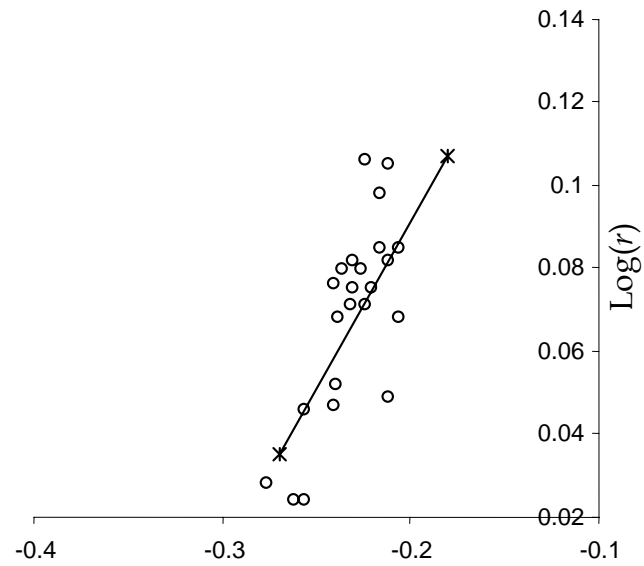
Figure 9: Comparison of experimental and calculated values of fluctuation ratio – Square bed



**Figure - 1**

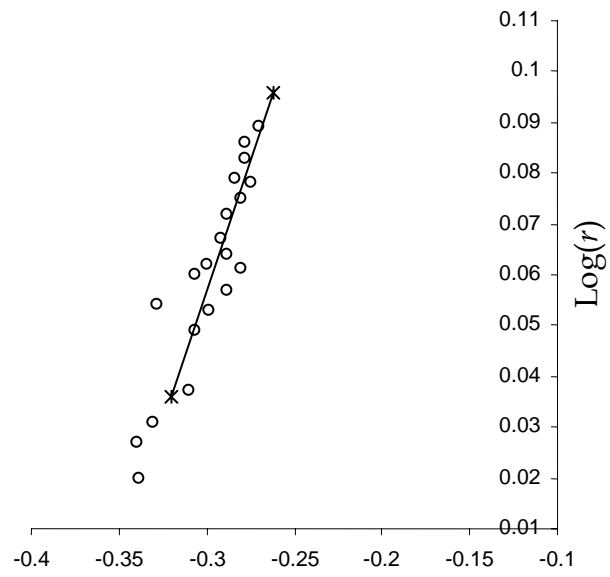
- |                     |                       |                       |
|---------------------|-----------------------|-----------------------|
| 1. Compressor       | 5. Line valve         | 9. Bed material       |
| 2. Receiver         | 6. Rotameter          | 10. Pressure tappings |
| 3. Silica gel tower | 7. Cylindrical column | 11. Manometer         |
| 4. Bypass valve     | 8. Glass bead packing | 12. Pressure gauge    |

Figure – 2



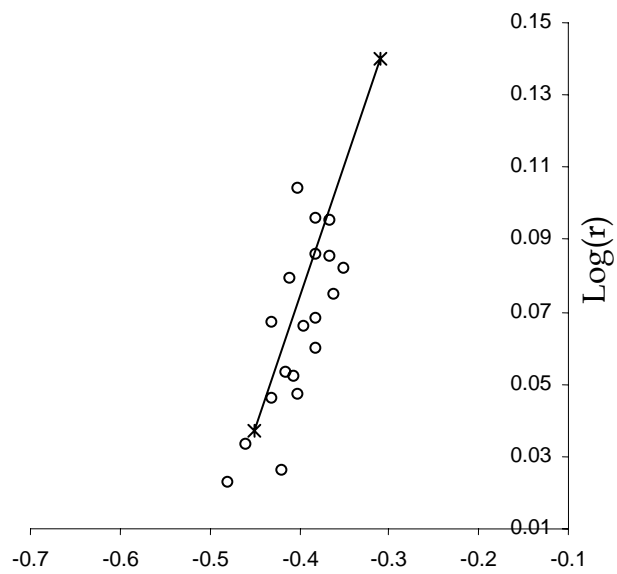
$$\text{Log} \left[ \left( \frac{dp}{Dc} \right)^{0.047} \left( \frac{Dc}{hg} \times \frac{\rho_f}{\rho_s} \right)^{0.039} \left( \frac{G_f - G_{mf}}{G_{mf}} \right)^{0.0591} \right]$$

Figure – 3



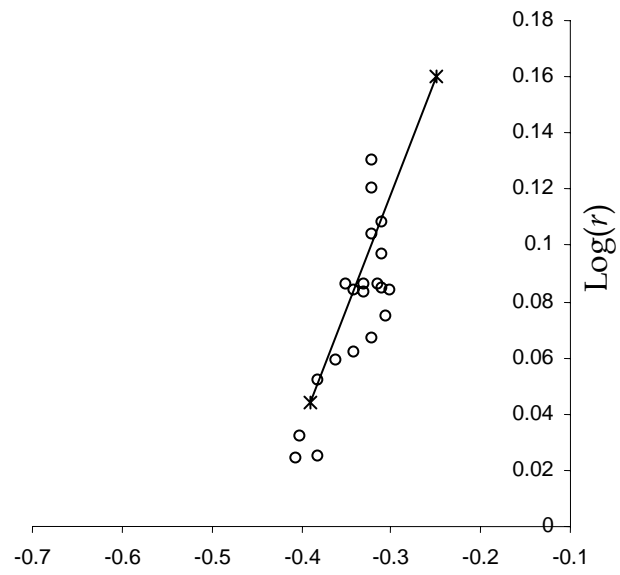
$$\text{Log} \left[ \left( \frac{dp}{Dc} \right)^{0.074} \left( \frac{Dc}{hg} \times \frac{\rho_f}{\rho_s} \right)^{0.039} \left( \frac{G_f - G_{mf}}{G_{mf}} \right)^{0.065} \right]$$

Figure – 4



$$\text{Log} \left[ \left( \frac{dp}{Dc} \right)^{0.0735} \left( \frac{Dc}{hg} \times \frac{\rho_f}{\rho_s} \right)^{0.0714} \left( \frac{G_f - G_{mf}}{G_{mf}} \right)^{0.08} \right]$$

Figure – 5



$$\text{Log} \left[ \left( \frac{dp}{Dc} \right)^{0.108} \left( \frac{Dc}{hg} \times \frac{\rho_f}{\rho_s} \right)^{0.05} \left( \frac{G_f - G_{mf}}{G_{mf}} \right)^{0.1} \right]$$



Figure – 6

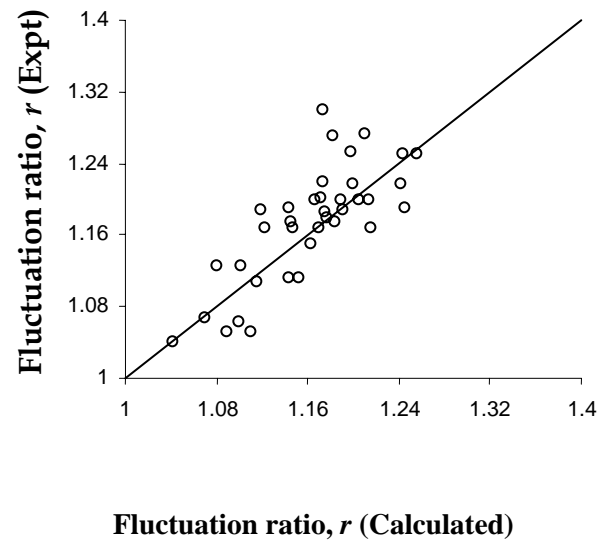


Figure – 7

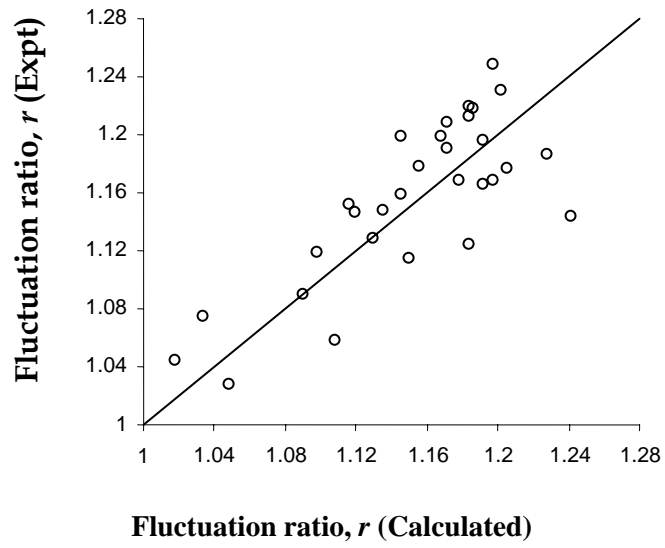


Figure – 8

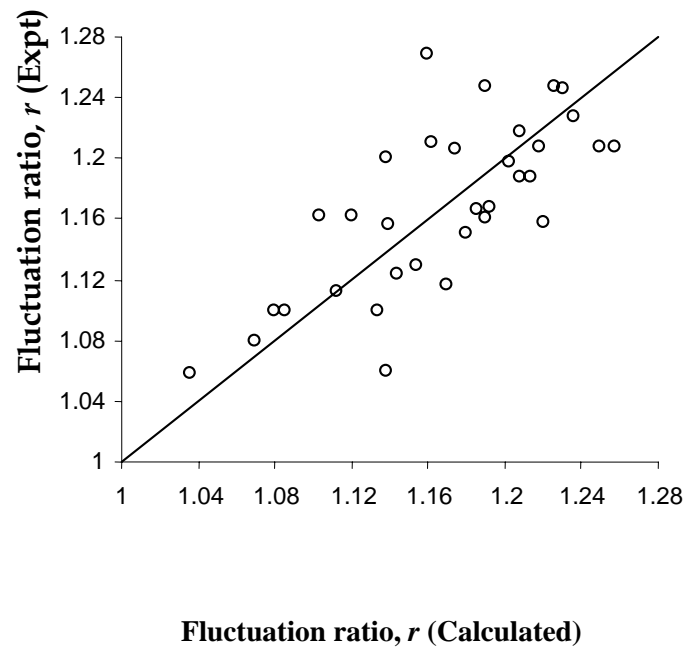


Figure - 9

